

Microfluidic Isolation of Leukocytes from Whole Blood for Phenotype and Gene Expression Analysis

Palaniappan Sethu,[†] Lyle L. Moldawer,[‡] Michael N. Mindrinos,[§] Philip O. Scumpia,[‡] Cynthia L. Tannahill,[‡] Julie Wilhelmy,[§] Philip A. Efron,[‡] Bernard H. Brownstein,^{||} Ronald G. Tompkins,[†] and Mehmet Toner^{*,†}

Surgical Services and Center for Engineering in Medicine, Massachusetts General Hospital, Harvard Medical School and Shriners Hospital for Children, Boston, Massachusetts 02114, School of Medicine, Washington University, St. Louis, Missouri 63101, Department of Surgery, University of Florida College of Medicine, Gainesville, Florida 32610, and Stanford Genome Technology Center, Palo Alto, California 94304

Technologies that enable the isolation of cell subtypes from small samples of complex populations will greatly facilitate the implementation of proteomics and genomics to human diseases. Transcriptome analysis of blood requires the depletion of contaminating erythrocytes. We report an automated microfluidic device to rapidly deplete erythrocytes from whole blood via deionized water lysis and to collect enriched leukocytes for phenotype and genomic analyses. Starting with blood from healthy subjects, we demonstrate the utility of this microfluidic cassette and lysis protocol to prepare unstimulated leukocytes, and leukocytes stimulated *ex vivo* with *Staphylococcal* enterotoxin B, which mimics some of the cellular effects seen in patients with severe bacterial infections. Microarrays are used to assess the global gene expression response to enterotoxin B. The results demonstrate that this system can isolate unactivated leukocytes from small blood samples without any significant loss, which permits more information to be obtained from subsequent analysis, and will be readily applicable to clinical settings.

A goal of modern clinical medicine is to develop high-throughput technologies to identify specific gene expression profiles of cells and tissues from individual patients and to correlate these profiles with particular disease outcomes. Indeed, the National Institute of General Medical Sciences (NIGMS) has established a Large Scale Collaborative Research Program (Inflammation and the Host Response to Injury; <http://www.gluegrant.org/>) whose principal goal is to ascertain the basis for different patient outcomes in response to trauma or burn injury. Leukocytes mediate the immune functions and contain information about the immediate inflammatory state of the body. A first step in this effort is to compile the expression profiles of blood leukocytes from trauma and burn patients at different clinical centers.

Leukocytes comprise only ~1.5% of the cells in total blood and must first be isolated from erythrocytes and reticulocytes before determining their transcriptome profiles. Currently, leukocyte

isolation is accomplished clinically via selective bulk lysis of erythrocytes or differential centrifugation. These macroscale methods are labor-intensive, nonstandardized, and require large samples. Furthermore, macroscale methods fail to efficiently isolate all leukocyte subpopulations and introduce variability via non-uniform conditions and extended times for mixing and diffusion. Indeed, analogous transcriptome results obtained from different laboratories and platforms are highly variable.^{1–3} Importantly, macroscale isolation stresses the cells for extended periods,^{4–8} which are known to activate leukocytes. Such activation alters gene and protein expression patterns, so these cells can be non-representative of those in the starting blood, which limits the usefulness of the information gained by analysis of this cell population.

Limitations of macroscale lysis for leukocyte isolation can be overcome by porting lysis to the microscale, via a device whose channel dimensions approximate blood cells. Such a device ensures rapid ionic diffusion and precise control and exposes each cell to uniform and gentle conditions⁹ so leukocyte phenotype and gene expression remain unperturbed. We previously explored the feasibility of using a microfluidics cassette, in conjunction with ammonium chloride lysis, to deplete erythrocytes from whole blood.⁹ While this device achieves shorter exposure times and increased leukocyte recoveries, its overall utility is limited: ammonium chloride requires greater than 40 s of exposure for complete erythrocyte lysis. Advantages of the microscale can be fully exploited by precisely controlling the exposure time to a few seconds, thereby achieving rapid lysis, minimizing activation, and processing sufficient sample to make the technique clinically applicable.

The current article describes the application of a new method, specifically the use of deionized water lysis to accomplish lysis of erythrocytes from whole blood. Lysis of erythrocytes in whole blood using deionized water without damage or activation of leukocytes is not possible in a macroscale system because of the

* Corresponding author. Phone: (617) 371-4883. Fax: (617) 523-1684. E-mail: mtoner@hms.harvard.edu.

[†] Harvard Medical School and Shriners Hospital for Children.

[‡] University of Florida College of Medicine.

[§] Stanford Genome Technology Center.

^{||} Washington University.

(1) Irizarry, R. A.; et al. *Nat. Methods* 2005, 2, 345–350.

(2) Steinmetz, L. M.; et al. *Nat. Rev. Genet.* 2004, 5, 190–201.

(3) Weis, B. K.; et al. *Nat. Methods* 2005, 2, 351–356.

(4) Fearon, D. T.; et al. *J. Immunol.* 1983, 130, 370–375.

(5) Glasser, L.; et al. *Am. J. Clin. Pathol.* 1990, 93, 662–669.

(6) Lundahl, J.; et al. *J. Immunol. Methods* 1995, 180, 93.

(7) Macey, M. G.; et al. *J. Immunol. Methods* 1995, 181, 211.

(8) Kouoh, F.; et al. *APMIS* 2000, 108, 417–421.

(9) Sethu, P.; Anahtar, M.; Moldawer, L. L.; Tompkins, R. G.; Toner, M. *Anal. Chem.* 2004, 76, 6247–6253.

inability of the macroscale environment to control exposure times on the order of 1–2 s. Though microfluidics approaches show potential for clinical application, their validation and actual application in clinical settings is not common. Preclinical validation of this technology to obtain useful functional genomics data from high-quality samples with predictive value for determination of patient outcomes has been demonstrated.

Here we report the first microfluidics cassette that achieves leukocyte enrichment without artifactual activation during processing. The leukocytes can be enriched from 0.6 mL of whole blood, via selective lysis of erythrocytes using deionized water in less than 10 s. We characterized this device by analyzing the recovered leukocytes using flow cytometry and transcriptome profiling and show that it eliminates several important shortcomings of the macroscale protocols that are in clinical use. Selective and quick erythrocyte lysis is achieved in a newly engineered cassette with microscale ridges that produce rapid mixing.¹⁰ This mixing ensures that every cell sees uniform conditions and enables the process to be scaled for a wide range of volumes of starting blood, with very efficient recovery of total leukocytes, and leukocyte subpopulations. Significantly, leukocytes undergo minimal stress and remain unactivated. To demonstrate the importance of isolation of unactivated leukocytes, we compare the expression profiles of naive leukocytes versus leukocytes stimulated with *Staphylococcus* enterotoxin B (SEB), which mimics cellular changes presented by individuals with bacterial infections, or early trauma. The results show that this method is repeatable and reliable without any artifactual activation, and the changes in gene expression following SEB stimulation can be easily identified.

MATERIALS AND METHODS

Blood Samples and Cell Activation. Blood collection was approved by the Institutional Review Board of the University of Florida College of Medicine. Twelve milliliters of blood was drawn from five healthy volunteers with heparin as anticoagulant (Vacutainer; Becton Dickinson, Franklin Lakes, NJ) and divided into two samples. One sample was divided into two aliquots and immediately processed by microfluidics, or by BD FACSLyse (BD Biosciences, San Jose, CA). The second sample was incubated at 37 °C for 2 h with 2 μ g/mL SEB (Sigma Fine Chemicals, St. Louis MO) to reprogram leukocyte gene and protein expression¹¹ and then divided into two aliquots for processing by microfluidics or FACSLyse.

Microfluidic Cassette Fabrication. The microfluidics device was fabricated using soft lithographic techniques. A silicon wafer was treated with oxygen plasma in an asher (March Instruments, Concord, MA) and spin coated with the negative photoresist SU-8 (MicroChem, Newton, MA). AutoCAD (Autodesk, Inc., San Rafael, CA) was used to generate a transparency mask (CAD ART Services Inc., Poway, CA) for photolithography, to create negative replicas of the channels. The elastomer poly(dimethylsiloxane) (PDMS; Dow Corning, Midland, MI) was mixed 10:1 with a cross-linker, poured on top the silicon wafer, and cured at 60 °C for 12 h. The elastomer with the replicated channels was released, and channel access holes were punched with a 22-gauge needle. The PDMS wafer was irreversibly bonded to a glass slide via oxygen

plasma. Access tubing (Tygon; Miami Lakes, FL) of slightly larger diameter was press-fitted into the holes.

Microfluidic Cassette Design and Operation. Figure 1 shows that the microfluidics cassette has three inlets and one outlet. The sample collection end has a sample outlet and an inlet for 2 \times phosphate-buffered saline (PBS) addition. The sample loading end has two inlets, for whole blood and for deionized water. Syringe pumps drive liquid flow, with blood at 20 μ L/min, and deionized water and 2 \times PBS at 600 μ L/min. Experiments were performed using a similar setup as described by Sethu et al.⁹ The water is divided into two streams that flank the whole blood stream leading into the serpentine lysis channel. At the flow rates used, the cells are in contact with deionized water for 10 s. Despite the limited time required for ionic diffusion in the microscale, the high concentration of blood cells may still produce nonuniform conditions, especially in the upstream microchannel. To rapidly and uniformly mix the cells, the channel floors are patterned with double herringbone microridges, which generate nonuniform resistance that effects fluid rotation. Also, the variable ridge length and their arrangement produce immediate chaotic mixing for even cell distribution. The channels are 160 cm long with cross section of 500 \times 200 μ m. Ridges are 25 μ m high and 20 μ m wide. Internal volume is 68.89 μ L.

Leukocyte Isolation and Recovery. Two 0.6-mL aliquots from the unstimulated and stimulated blood samples were enriched for leukocytes via microfluidic lysis or via the widely used FACSLyse protocol, which lyses erythrocytes using hypertonic conditions in macroscale for 5 min and fixes the remaining leukocytes for flow cytometry. The device processes 20 μ L of blood/min, so 0.6 mL requires 30 min. Note that each blood cell is exposed to the hypotonic lysis conditions in the cassette device for just 8–10 s. The procedure requires no user assistance, is fully automated, and can be run in parallel.

Figure 1 shows whole blood and deionized water are simultaneously introduced into the cassette via their respective inlets, to achieve a 1:30 blood-to-deionized water ratio, which we determined produces complete erythrocyte lysis within 10 s. Based on channel dimensions, a 600 μ L/min flow rate gives a 10–12-s cell residence time. At the cell collection end, 2 \times PBS, with or without 2% paraformaldehyde (Fisher Scientific Corp., Pittsburgh, PA), quickly returns the cells to isotonic conditions, for flow cytometry and RNA isolation, respectively. Lysed samples, enriched for leukocytes, are collected from the outlet in 0.5-mL Eppendorf tubes, with cell debris removed in the supernatant by low-speed centrifugation. The leukocyte pellets are washed and dispersed in 1 \times PBS for subsequent analyses.

Leukocyte Phenotyping. For each leukocyte-enriched sample, total cell recovery was measured by hemocytometry; and different subpopulations were assessed by flow cytometry (FACSCalibur, Becton Dickinson). Cells were stained using BD FastImmune (BD Biosciences, San Jose, CA). Lymphocyte cell surface markers were visualized using peridin chlorophyll-a (PerCP)-conjugated anti-CD3, fluorescein isothiocyanate (FITC)-conjugated anti-CD4, and phycoerythrin (PE)-conjugated anti-CD69. Monocyte and platelet markers were visualized using FITC-anti CD36, PE-anti CD11b, PerCP-anti MHC class II, and APC-anti CD18. Neutrophil markers were visualized using FITC-anti CD66b, PE-anti CD11b, and APC-anti CD18. Also, APC-anti CD19 and APC-anti CD56 were

(10) Stroock, A. D.; et al. *Science* **2002**, *295*, 647–651.

(11) Feezor, R. J.; et al. *Physiol. Genomics* **2004**, *19*, 247–254.

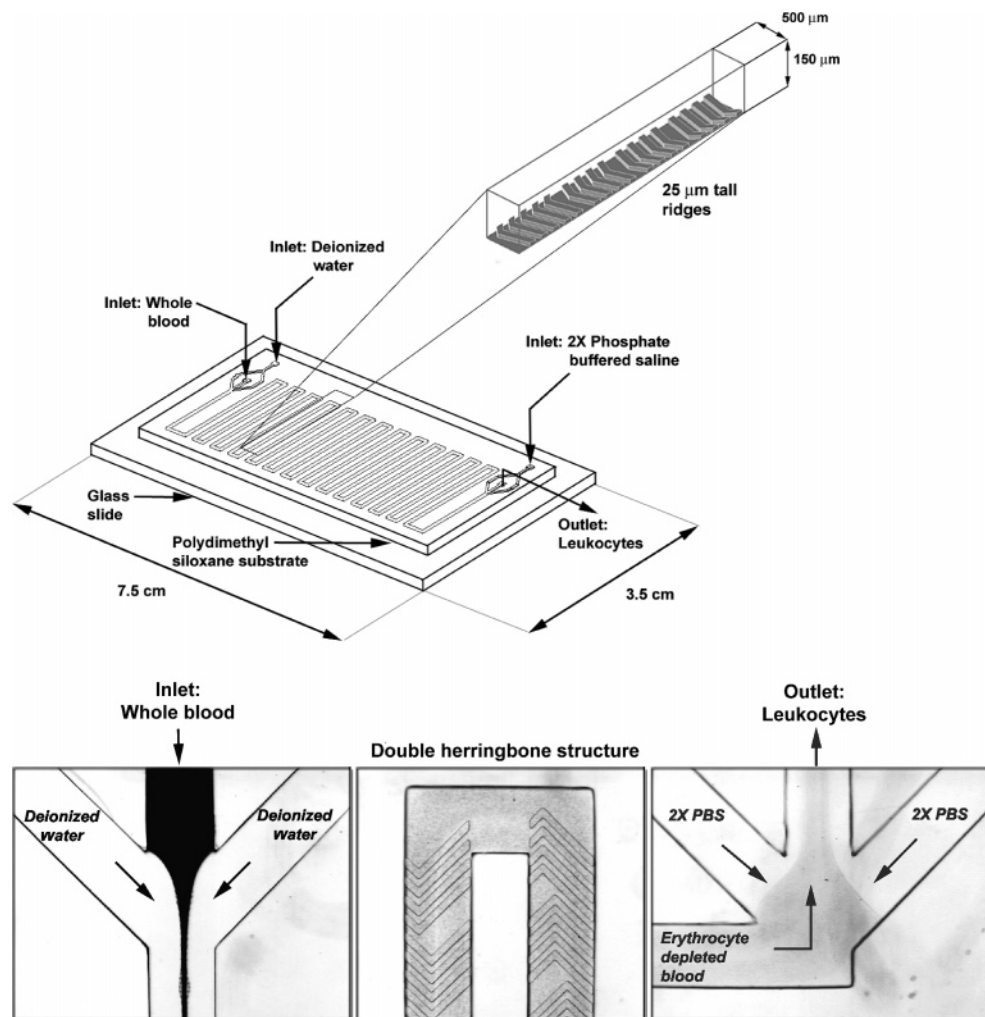


Figure 1. Microfluidic lysis cassette. Device design and construction to facilitate the rapid lysis of erythrocytes and isolation of leukocytes following erythrocyte lysis. The bottom panel shows different locations in the cassette. (A) Inlets for addition of whole blood sample and deionized water. (B) The double herringbone structures in the microchannel floor mediate chaotic mixing and uniform cell distribution. (C) Outlets for addition of 2× PBS to restore isotonic conditions and to collect erythrocyte depleted leukocyte samples. The samples and reagents are automatically metered out in precise predetermined volumes, and the constant flow conditions prevent sedimentation or cell loss in the microchannels. Complete and rapid mixing of the cells with the lysis buffer streams were visually confirmed by microscopy.

respectively used to identify B and NK cells. Stained cells were washed in 1% Hank's balanced salts (HAB) without calcium or magnesium, plus 1% bovine serum albumin, 0.1% sodium azide, and 1 mM ethylenediaminetetraacetic acid), pelleted, resuspended in HAB, and analyzed on a FACSCalibur flow cytometer (BD Biosciences), using CellQuest software (BD Pharmingen). Cell activation was scored using unpaired Student's *t*-tests with the two-tailed significance $p < 0.05$. Rank Sum Tests were performed when equal variance failed between the two groups. All data correspond to the means of cell concentration or fluorescence intensity, \pm SD, for $n = 5$.

cRNA Synthesis and Microarray Hybridization. Washed leukocytes were immediately lysed in 600 μ L of RLT (Qiagen, Hilden, Germany), 1% v/v β -mercaptoethanol and stored at -80°C . Total RNA was isolated using the RNeasy Mini Kit (Qiagen), with DNA removed by on-column DNase digestion. Quality and purity of total RNA and biotinylated, synthesized cRNA were determined by capillary electrophoresis using the Bioanalyzer 2100 system (Agilent, Palo Alto, CA). cRNA was amplified¹² from 1 μ g of total RNA. cRNA was transcribed in vitro incorporating

biotinylated nucleotides using the Affymetrix High Yield RNA Transcript T7 Kit (Affymetrix, Inc., High Wycombe, UK) and the product hybridized onto an Affymetrix HGU133 plus GeneChip for 16 h at 45°C in an Affymetrix hybridization oven. Arrays were stained and washed using an Affymetrix fluidics station and EukGEWSv4 Affymetrix protocol and analyzed on an Affymetrix scanner.

Microarray Data Analysis and Biostatistics. Low- and high-level statistics were performed using dChip (Wong Laboratory, Department of Biostatistics, Harvard School of Public Health). Expression was modeled using the perfect match only dChip algorithms.¹³ Affymetrix Microarray Suite Gene Chip Operating Software identified probe sets as "absent" whose signal intensities were at or below background. Absent probe sets on all arrays were discarded from the high-level analysis.

An unsupervised analysis was applied to assess similarities and gene expression profile differences. A variation filter identified probe sets exhibiting a coefficient of variation of >0.5 across the

(12) Gelder, R. N. V.; et al. *Proc. Natl. Acad. Sci. U.S.A.* **1990**, *87*, 1663–1667.
(13) Li, C.; Springer, NY, 2003.

entire data set. The mean-centered and variance-normalized levels were then subjected to principal component and hierarchical cluster analyses using the dChip algorithm. Pearson's correlation coefficient¹⁴ was calculated to assess similarity of gene expression among probe sets, with the results displayed as a dendrogram on top of the cluster image. Significance analysis of microarrays identified probe sets in which intensities differ between the two groups at a false discovery rate of 1% ($B = 0.01$).¹⁵

RESULTS

Microfluidics Cassette and Water Lysis Increases Recovery of Leukocytes and Subpopulations. Leukocytes comprise ~1.5% total human blood cells, so whole blood must be depleted of erythrocytes before assessing phenotype and gene expression of leukocyte subpopulations. The macroscale FACSlyse protocol, which is widely used in clinical laboratories to enrich leukocytes from whole blood for cell sorting, mediates selective erythrocyte depletion via hypertonic lysis for 5 min in bulk. Erythrocytes lyse fastest by exposure to deionized water. To selectively lyse erythrocytes in whole blood via hypotonic conditions, while minimizing cell exposure, we determined 30× deionized water for 1 μ L of whole blood mediates complete erythrocyte lysis in 8 ± 1 s, while lymphocyte, monocyte, and granulocyte lysis respectively begin at 32 ± 5 , 372 ± 26 , and 84 ± 7 s. Based on these results, we engineered the microfluidic cassette shown in Figure 1. With this device, each cell is uniformly exposed to deionized water for 8–10 s before returning to isotonic conditions. Furthermore, the cassette channels contain microscale ridges that produce very rapid mixing and uniform exposure of each cell to the lysis conditions. This system significantly reduces chemical and mechanical cell stresses during processing.

Beginning with whole blood from five healthy subjects, we collected and analyzed five sets of enriched leukocyte samples using the microfluidics cassette or the FACSlyse protocol. Figure 2 demonstrates that the microfluidics system is superior to macroscale lysis for both total and differential leukocyte recovery, as assessed by hemocytometry, and flow cytometry for diagnostic cell surface markers. Indeed, from the same volume of whole blood, the microfluidics cassette yields >25% more total leukocytes versus FACSlyse. Furthermore, microfluidics lysis significantly improves differential recoveries of CD3⁺ lymphocyte and CD36⁺ monocyte cell subpopulations; thus, the leukocytes isolated using microfluidics versus macroscale lysis are more representative of the leukocyte cell population in starting blood samples due to preservation of all subpopulations.

Differential Expression of Surface Activation Markers via Microscale versus Macroscale Lysis. Two-hour exposure of whole blood to SEB dramatically reprograms gene and protein expression in leukocyte cell subpopulations.¹¹ SEB binds to class II major histocompatibility complex proteins to activate V β -expression T-lymphocytes, stimulate T lymphocyte proliferation, increase the synthesis of proinflammatory cytokines in T-cells and monocytes,^{16,17} and activate granulocytes and monocytes via T-cell secreted IL-1 β , IL-2, and IFN- γ . These changes mirror many of the cellular and molecular changes in patients with bacterial infections or early trauma.^{18,19} While clinical analysis of the

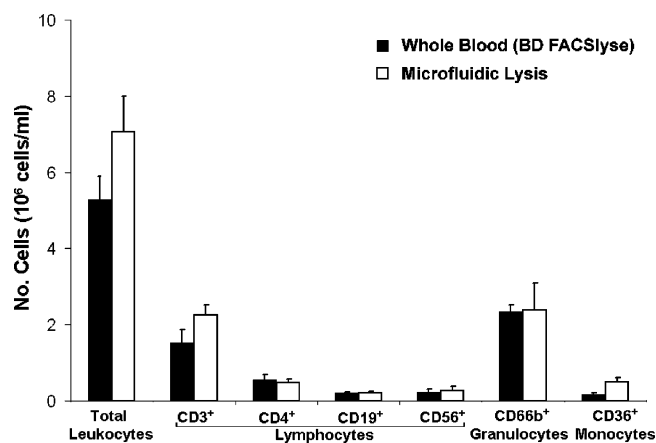


Figure 2. Microfluidics lysis effect on total and differential leukocyte recoveries. Leukocyte recovery and differential cell counts were respectively determined by hemocytometry and by staining for cell surface markers and flow cytometry analysis. Leukocyte samples isolated following hypotonic lysis of whole blood using the microfluidic cassette versus the BD FACSlyse protocol are compared. No apparent loss of any cell subpopulation following erythrocyte lysis is seen for the microfluidics samples. The results are summarized from the data obtained from the five different starting blood samples.

activation state of leukocyte subpopulations in such patients could facilitate their treatment,²⁰ current leukocyte isolation methods can themselves artifactually activate leukocytes.^{4–8} To this end, we isolated and characterized leukocytes from naive whole blood, and whole blood stimulated with SEB, to demonstrate that the microfluidics cassette provides cells representative of leukocyte subpopulations in blood prior to processing.

Naive and SEB-stimulated samples were lysed in the cassette, with the enriched leukocytes fixed on chip for phenotypic analyses. The activation status of each sample, versus those of naive and SEB cells isolated via whole blood lysis, was analyzed by flow cytometry: the samples were stained and sorted for constitutive cell surface markers for T-lymphocytes (CD3⁺ CD4⁺), monocytes (CD36⁺), and granulocytes (CD66b⁺), together with early activation markers for these subpopulations. Figure 3 presents these activation data, which are summarized in Table 1 for the five starting blood samples, expressed as percentage of cells expressing high levels of the activation markers.

CD69 is diagnostic of activated T helper cells. Table 1 shows that only ~1% of the naive cells exhibit high CD69 levels, and upon stimulation, the microfluidics-isolated T-cells, but not those from the macroscale method, have statistically more cells with high CD69 levels. Similarly, the integrins CD11b and CD18 are constitutively expressed at low levels on monocytes and granulocytes and are upregulated following SEB stimulation or cell stress.²¹ For monocytes, CD11b, CD18, and human leukocyte antigen-DR (HLA-DR) significantly increase with SEB exposure in the microfluidics samples. In contrast, only HLA-DR is significantly upregulated in the macroscale samples. Indeed, the corresponding naive cells exhibit high CD11b and CD18 levels that are statistically equivalent to those seen in the SEB microscale and macroscale samples, indicating macroscale protocol isolation

(14) Eisen, M. B.; et al. *Proc. Natl. Acad. Sci. U.S.A.* **1998**, *95*, 14863–14868.
 (15) Tusher, V. G.; et al. *Proc. Natl. Acad. Sci. U.S.A.* **2001**, *98*, 5116–5121.
 (16) Trede, N. S.; et al. *Clin. Immunol. Immunopathol.* **1994**, *70*, 137–144.
 (17) Schramm, R.; et al. *Infect. Immun.* **2003**, *71*, 2542–2547.

(18) Feezor, R. J.; et al. *Clin. Infect. Dis.* **2005**, *41*, S427–S435.
 (19) Biberthaler, P.; et al. *Shock* **2005**, *24*, 11–19.
 (20) Cobb, J. P.; et al. *Proc. Natl. Acad. Sci. U.S.A.* **2005**, *102*, 4801–4806.
 (21) Rebuck, N.; et al. *FEMS Immunol. Med. Microbiol.* **1994**, *8*, 189–195.

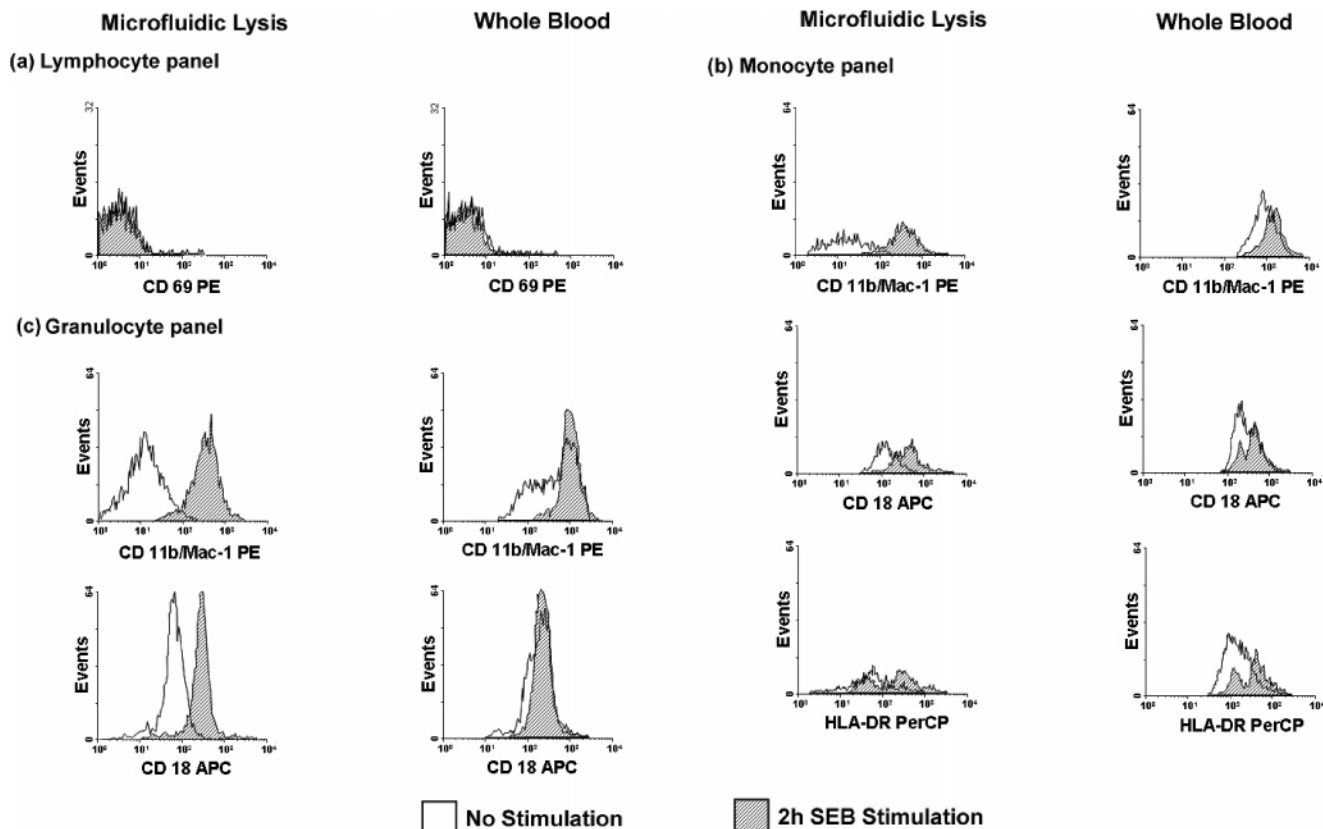


Figure 3. Reduction of leukocyte activation by microfluidic lysis. Leukocytes \pm ex vivo SEB stimulation were isolated using the microfluidic cassette or whole blood lysis, to produce five sample sets that were stained for cell surface markers and analyzed by cell sorting. Cell events were scored based on forward and side fluorescence scatter. (a) T helper lymphocytes were identified by CD 3⁺ and CD 4⁺ staining, with activated cells also staining for increased CD 69 expression. (b) Monocytes were identified by CD 36⁺ staining, with the state of activation assessed via increased CD 11b, CD 18, and HLA-DR expression. (c) Granulocytes were identified by CD 66b⁺ staining, with the state of activation assessed via increased CD 11b and CD 18 expression. High expression levels of the activation markers demonstrate cell activation. Data are shown for a single representative whole blood sample. Table 1 summarizes the results for all five of the whole blood samples that were collected and analyzed.

Table 1. Expression of Cell Surface Activation Markers + SEB Stimulation^a

	(a) microfluidic lysis (%)		(b) whole blood (%)	
	no stimulation	2-h SEB stimulation	no stimulation	2-h SEB stimulation
T helper cells CD4 CD69 ^{high}	1.56 \pm 0.54	9.27 \pm 5.75 ^b	1.24 \pm 0.46	5.69 \pm 4.16 ^b
monocytes CD36 ⁺ CD11b Mac-1 ^{high}	4.55 \pm 3.60	73.69 \pm 6.15 ^b	39.09 \pm 17.27	39.20 \pm 17.68
monocytes CD36 ⁺ CD18 ^{high}	0.99 \pm 0.48	37.81 \pm 17.52 ^b	27.32 \pm 10.32	13.43 \pm 9.55
monocytes CD36 ⁺ HLA-DR ^{high}	5.48 \pm 2.72	20.44 \pm 13.22 ^b	14.99 \pm 1.17	43.72 \pm 17.88 ^b
granulocytes CD66b ⁺ CD11b/Mac-1 ^{high}	3.05 \pm 3.91	80.50 \pm 6.89 ^b	25.36 \pm 16.31	28.80 \pm 25.14
granulocytes CD66b ⁺ CD18 ^{high}	1.29 \pm 0.72	68.11 \pm 22.71 ^b	8.29 \pm 3.11	9.18 \pm 9.30

^a Summary of expression levels of cell surface activation markers on leukocytes isolated using the microfluidics cassette versus whole blood (FACSlyse) lysis are presented. Early activation markers were used to score in vivo activation of CD 4⁺ T lymphocytes, CD 36⁺ monocytes, and CD 66b⁺ granulocytes. Data are presented as percentages \pm SD for sample size $n = 5$. Asterisks denote samples where SEB stimulation causes a significant increase ($p < 0.05$) in expression of the respective activation marker. ^b No stimulation versus 2-h SEB stimulation.

partially activates cells. Granulocytes give equivalent results; only the microfluidics samples exhibit CD11b and CD18 induction to SEB. Note that up to 80% of the monocyte and granulocyte cells are activated within 2 h of SEB exposure. This activation could play a significant role in the early pathology of the host response to severe infection.

The microfluidics cassette clearly achieves leukocytes that much better reflect the unactivated state of leukocytes in the initial whole blood sample versus those leukocytes using the macroscale isolation. Indeed, the surface markers on the microfluidics cells

remain unactivated to a much higher degree than cells from whole blood lysis. Furthermore, the microfluidics cells exhibit much greater differences in cell surface activation markers when comparing samples unstimulated and stimulated with SEB. These differences likely are the product of the rapid lysis and on-chip fixation steps and demonstrate the microfluidics system much better provides unactivated leukocytes from whole blood samples versus macroscale methods, which partially activate naive leukocytes and, furthermore, suppresses their subsequent response to ex vivo SEB stimulation.

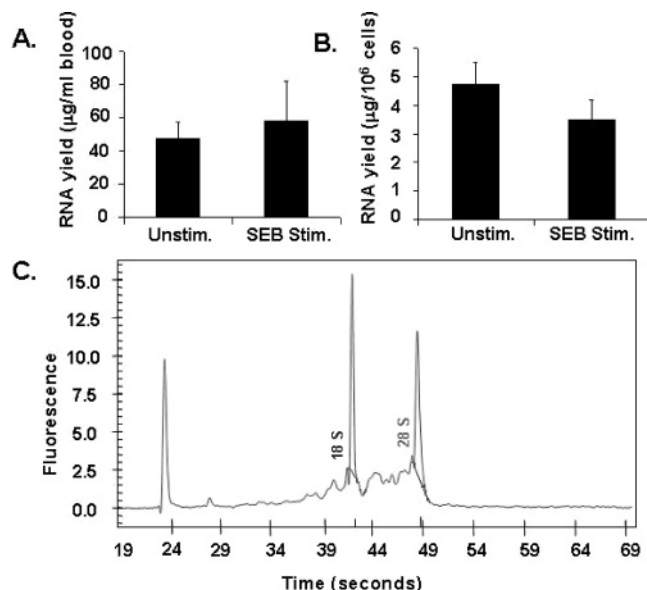


Figure 4. Efficient yield and high quality of RNA from cells isolated via microfluidics lysis. (A) RNA yield expressed as $\mu\text{g/mL}$ of blood processed and (B) RNA yield expressed as $\mu\text{g}/10^6$ isolated leukocytes. RNA was isolated using RNeasy (Qiagen). RNA quantity did not differ when the blood was stimulated ex vivo with SEB. (C) RNA quality was assessed by capillary electrophoresis. The distinct 28S and 18S peaks and the low baseline demonstrate the RNA is undegraded.

Transcriptome Analysis of Microfluidics-Isolated Leukocytes. A goal of clinical genomics research is to determine the global gene expression profiles of particular blood cell subpopulations in individual patients and to correlate these profiles with different outcomes. To this end, we isolated RNA for microarray analysis from the unstimulated and SEB-stimulated leukocyte samples prepared using the microfluidics cassette. As determined by capillary electrophoresis, leukocyte RNA isolated from 0.6 mL of starting whole blood was of high quality and of similar quantity for the unstimulated and SEB-stimulated samples (Figure 4).

SEB stimulation dramatically alters leukocyte gene expression.^{11,22} We reassessed gene expression changes in response to ex vivo SEB exposure in leukocytes isolated via the microfluidics cassette and water lysis. The unsupervised analysis in Figure 5 shows 2489 probe sets, whose mRNA abundance had a coefficient of variance of $>50\%$. Hierarchical clustering of these sets shows that all four replicate naive samples cluster on one side of the dendrogram, with the four stimulated samples on the other (Figure 5A). The degree of correlation, estimated by the length of the dendrogram branches determined by Pearson's correlation coefficient, is 0.98 ± 0.01 , demonstrating a strong linear relationship. Clearly, the mRNA abundance from these replicate naive samples more closely correlated with each other than they are to the stimulated samples, and vice versa, showing that subject variability is markedly less than the differences in mRNA abundance produced by ex vivo stimulation. Figure 5 presents a principal

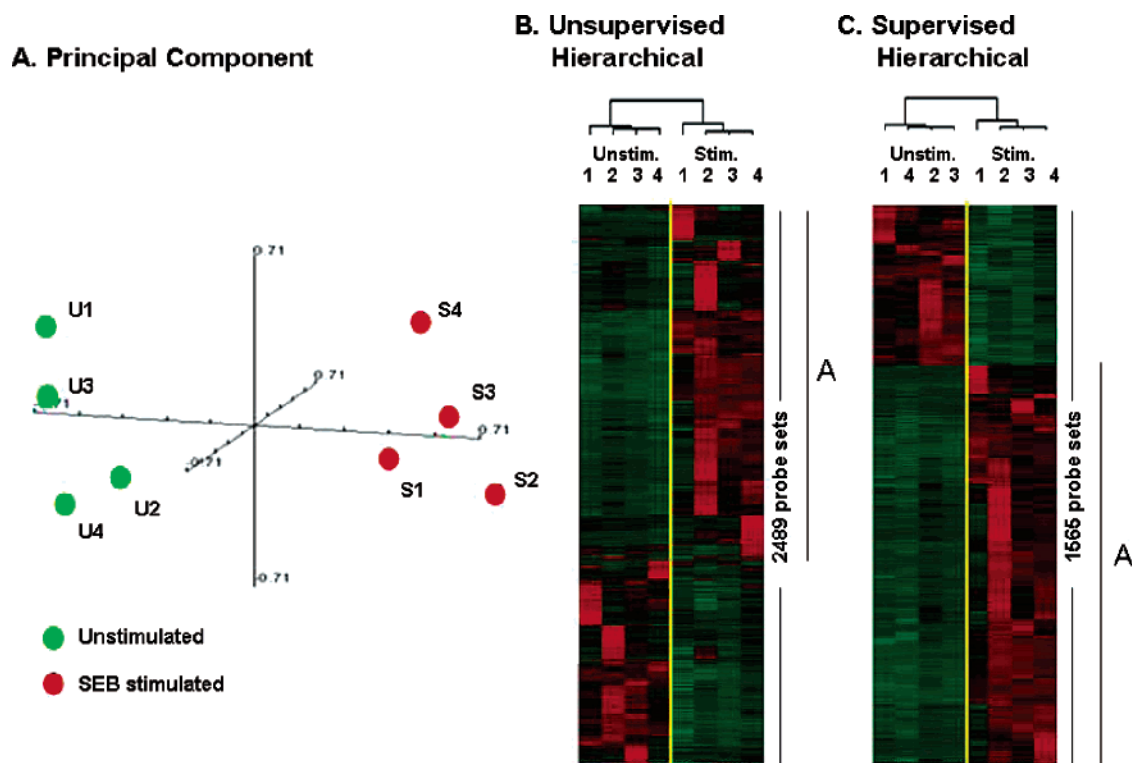


Figure 5. Principal component and hierarchical cluster analyses of leukocyte genes differentially expressed minus and plus SEB. Using the microfluidics cassette, leukocytes were isolated from four naïve blood samples or from the four corresponding blood samples following 2-h ex vivo SEB stimulation. Total RNA was prepared and transcript abundance determined by hybridization to the Affymetrix U133 Plus 2 GeneChip. (A) Principal component analysis of 2489 probe sets whose expression is above baseline and normalized variation coefficient of >0.5 . (B) Unsupervised hierarchical clustering of these same probe sets. (C) Supervised hierarchical clustering by SAM analysis of 1535 probe sets whose expression differs between the naïve and SEB-stimulated samples at a 0.01 false discovery rate. In the cluster analyses, (A) corresponds to probe sets whose expression is up-regulated by SEB exposure. Unstim, naïve leukocytes; Stim, SEB-stimulated leukocytes. Both the supervised and unsupervised analyses demonstrate the naïve samples cluster with each other, and the stimulated samples cluster together separately.

Table 2. Highest Expressed Genes in Unactivated Leukocytes^a

probe sets	gene name	gene symbol	molecular function
200801_x_at			
213867_x_at	actin, b	b-actin	cytoskeleton, actin filament
224594_x_at			
214370_at	calgranulin A	S 100AS	calcium ion binding
202917_sat			
200031_sat	ribosomal protein S11	RPS11	rRNA binding
213350_at			
201492-s-at	ribosomal protein L41	RPL41	ribosomal protein synthesis
200949_x-at216246_at	ribosomal protein S20	RPS20	ribosomal protein synthesis
214003_x_at			
204892_x_at	eukar elongation factor-1 al	EEF1A1	translation elongation
206559_x_at			
213477_x_at200963-x_at	ribosomal protein L31	RPL31	ribosomal protein synthesis
200888_sat	ribosomal protein L23	RPL23	ribosomal protein synthesis
200909-sat	ribosomal protein large P2	RPLP2	RNA binding
210646 -x-at			
210646_x_at	ribosomal protein L13a	RPL13a	ribosomal protein synthesis
200716-x_at			
200674_sat	ribosomal protein L32	RPL32	ribosomal protein synthesis
202029_x_at	ribosomal protein L38	RPL38	ribosomal protein synthesis
217733_sat	thymosin, b10	TMSB 10	actin binding, cytoskeletal
200748-sat	ferritin heavy polypeptide 1	FTH1	ferroxidase activity, iron binding
214143-x_at	ribosomal protein L24	RPL24	ribosomal protein synthesis
217028-at	chemokine (CXC) receptor 4	CXCR4	chemokine receptor activity
216438-s-at	thymosin, β 4 X-linked	TMSBXL	actin binding cytoskeletal
208825 -x-at	ribosomal protein L23a	RPL23A	ribosomal protein synthesis
208834-x-at201094-at	ribosomal protein S29	RPS29	ribosomal protein synthesis
221700-s-at	ubiquitin A-52 residue ribosomal protein fusion product 1	UBA52	ribosomal protein synthesis
201429-s5_at	ribosomal protein L37a	RPL37A	ribosomal protein synthesis
231735-sat	PRO 1073 protein	PRO1073	hypothetical protein
200095_x_at	ribosomal protein SO10	RPS10	ribosomal protein synthesis
200092-s-at	ribosomal protein L37	RPL37	ribosomal protein synthesis
213356_x_at	heterogeneous nuclear	HNRNPA1	nucleotide binding
200016_x_at	ribonucleoprotein A1		ribosomal protein synthesis
203034-s_at	ribosomal protein L27	RPL27	
212869-x-at	turn or protein	TPTC1	translationally controlled
1553570-x-at	unknown		

^a The highest expressed probe sets in unstimulated leukocytes isolated from whole blood using the microfluidics lysis cassette are listed. The most abundant genes are structural and associated with the cell skeleton, such as actin or thymosin, or encode ribosomal proteins. Note the absence of hemoglobin genes, which demonstrates the lack of erythrocyte and reticulocyte contamination.

component plot comparing gene expression results for unstimulated versus SEB stimulated leukocytes. These results demonstrate some modest variation between the replicate samples but dramatic differences between the unstimulated and SEB stimulated groups.

Table 2 lists the most highly expressed genes in unstimulated leukocytes. As expected, these genes predominantly encode proteins involved in synthesis and cell cytoskeleton maintenance functions. The most abundant transcripts in unprocessed whole blood are globin isoforms¹¹ and platelet-specific functions. Here, hemoglobin¹¹ and platelet-associated^{23,24} transcripts are noticeably absent from the transcriptome profiles, demonstrating the efficiency of microfluidics lysis to deplete erythrocytes, reticulocytes, and platelets.

To identify genes whose mRNA abundance is most altered by SEB, a supervised analysis was performed using a two-class comparison on the total unlogged data set. The expression of 1565

probe sets, significantly differed between the naive and stimulated samples, with a false discovery rate of <1% (Figure 5B). Table 3 lists genes whose mRNA abundance is most up- or downregulated. Upregulated genes encode inflammatory functions, including interleukins (IL-1 α , IL-1 α), chemokines (CCL2, CCL8, CCL20, CXCL3, CXCL10, CXCL11), and cell surface receptors (ICAM1, CD83). At the same time, a reprioritization of gene expression occurs, and many genes whose expression declines have unknown identities or functions or encode general activities.

DISCUSSION

High-throughput genomic technologies should revolutionize the treatment of human disease. For example, trauma patients display differential outcomes ranging from full recovery to sepsis, multisystem organ failure, and death. These outcomes reflect different host responses to injury, such as overexpression of inflammatory activities. Direct assessment of global leukocyte gene expression should provide insights into the pathological basis of trauma and the development of individualized treatment regimens. Routine profiling of individual patients remains unreli-

(22) Mendis, C.; et al. *TY-JOUR* **2005**, *6*, 84–94.

(23) Gnatenko, D. V.; et al. *Blood* **2003**, *101*, 2285–2293.

(24) McRedmond, J. P.; et al. *Mol. Cell. Proteomics* **2004**, *3*, 133–144.

Table 3. Highest Upregulated and Downregulated Genes in Response to SEB Stimulation^a

probe set	gene name	gene symbol	molecular function	fold change (SEB/control)
(a) Upregulated Genes				
210118-sat	interleukin-1 α	IL1A	inflammatory, immune response	118.7
223484_at	normal mucosa of esophagus specific 1	NMES1	nucleus, unknown function	90.6
204533_at	chemokine (C-X-C motif) ligand 10	CXCL10	immune response, chemotaxis	82.4
205207_at	interleukin-6	IL-6	acute phase response	78.4
216598_sat	chemokine (C-C motif) ligand 2	CCL2	immune response, chemotaxis	63.5
216243_sat				63.5
216245_at	interleukin-1 receptor antagonist	IL1RN	inflammatory response	54.9
212659_sat				42.6
223767_at	G protein coupled receptor 84	GPR84	G protein receptor activity	50.8
214038_at	chemokine (C-C motif) ligand 8	CCL8	immune response, chemotaxis	50.4
209959_at	nuclear receptor subfamily 4, A3	NR4A3	steroid hormone receptor activity	49.1
1563118_at	CDNA FLJ20923 fis	FLJ20923	hypothetical protein	44.9
240287_at	similar to immune-responsive gene 1	LOC341720	hypothetical protein	44.4
210004_at	oxidized LDL (lectin-like) receptor 1	OLR1	receptor activity, sugar binding	43.3
205476_at	chemokine (C-C motif) ligand 20	CCL20	immune response chemotaxis	42.6
211434_s-at	chemokine (C-C) receptor-like 2	CCR2L	immune response, chemotaxis	41.6
210354_at	Interferon-gamma	IFNG	immune response	37.9
206932_at	cholesterol 25-hydroxylase	CH25H	lipid metabolism, catalytic activity	35.8
204363_at	thromboplastin (tissue factor)	F3	blood coagulation, immune response	34.8
240103_at	CDNA FLJ20923	FLJ20923	hypothetical protein	32.5
36711_at	v-maf homolog F	MAFF	transcriptional regulator	30
205067_at	interleukin-1 β	IL1B	inflammatory, immune response	30
210163_at	chemokine (C-X-C motif) ligand 11	CXCL11	immune response, chemotaxis	28
202637_s-at	intercellular adhesion molecule 1(CD54)	ICAM1	cellular adhesion, immune response	27.7
206115_at	early growth response 3	EGR3	transcriptional regulator	24.9
217996_at	pieckstrin domain. family A, member 1	PHLDA1	nucleus. unknown function	24
207850_at	chemokine (C-X-C motif) ligand 3	CXCL3	immune response. chemotaxis	22.6
(b) Downregulated Genes				
241631_at	zinc finger protein 219	ZFP219	transcriptional regulator	0.06
237954_x-at	0.1			
242179_s-at	tetraspanin 16		integral membrane protein	0.07
233236_at				0.18
209864_at	frequently rearranged in advanced T-cell lymphomas 2	FRAT2	receptor. Wnt signaling pathway	0.09
217521_at	histidine ammonia-lyase	HAL	histidine. amino acid metabolism	0.1
238363_at	catalase	CAT	oxidoreductase activity	0.1
241627_x_at		FLJ10357	hypothetical protein	0.1
219666_at	membrane-spanning 4-domains, subfamily A. member 6A	MS4A6A	receptor, signal transduction	0.12
214058_at	v-myc myelocytomatosis viral oncogene homologue 1	MYCL1	transcription factor activity	0.12
222760_at	hypothetical protein FLJ14299	FLJ14299	hypothetical protein	0.14
229382_at	hypothetical protein LOC284465	LOC284465	hypothetical protein	0.15
233217_at	HSPC102	HSPC102	hypothetical protein	0.15
226657_at	hypothetical protein DKFZp762H185	DKFZp762H185	hypothetical protein	0.15
212993_at	mRNA. cDNA DKFZp667B1718	DKFZp667B1718	hypothetical protein	0.16
229383_at	membrane-associated ring finger 1	MARCH1	ubiquitin protein ligase activity	0.16
1560169_at	chromosome 9 open reading frame42	C90RF42	unknown function	0.17
228791_at	hypothetical protein MGC61550	MGC61550	hypothetical protein	0.18
1553311_at	hypothetical protein FLJ33860	FLJ33860	hypothetical protein	0.18
230586_sat	hypothetical protein FLJ14299	FLJ14299	hypothetical protein	0.18
232077_sat	yippee-like 3 (<i>Drosophila</i>)	YPYL3	unknown function	0.19
209841_sat	leucine rich repeat neuronal 3	LRRN3	nucleus. unknown function	0.2
219242_at	centrosome protein Cep63	Cep63	centrosome. unknown function	0.2
225177_at	RAB11 family interacting protein 1	RAB11FIP1	unknown function	0.2
1568934_at	chemokine (C-X3-C motif) receptor 1	CX3CR1	chemotaxis. cell defense	0.21
220987_sat	chromosome 11 open reading frame 17	C11ORF17	unknown function	0.21
229114_at	GRB2-associated binding protein 1	GAB1	SH3/SH2 adaptor activity, EGFR pathway	0.21

^a The 25 genes whose expression increases or decreases the greatest in response to ex vivo SEB stimulation are listed. (a) Upregulated genes encode inflammatory proteins (IL-1 α , IL-1 β), chemokines (CCL2, CCL8, CCL20, CXCL3, CXCL10, CXCL11), or cell surface receptors (ICAM1, CD83). (b) Fifteen out of 25 of the most downregulated genes encode hypothetical proteins with unknown functions. Known genes encode transcriptional regulatory or cell-signaling functions.

able, as current leukocyte isolation protocols can perturb gene expression, require large starting blood volumes, lead to selective

loss of leukocyte subpopulations, and are variable and unsuitable for clinical settings. The ideal leukocyte profiling system should

enable the input of whole blood samples at one end and the output of molecular data at the other. For clinical use, such a system must be standardized, automated, fast, and efficient and achieve robust and reproducible results with high signal-to-noise ratios. This system could include components that achieve erythrocyte removal via selective lysis, isolation of leukocyte subpopulations via panning, efficient isolation of total RNA, and RNA hybridization to a microarray to query the quantitative expression of the complete human genome. Here we report a device that achieves the initial isolation step of such a system and demonstrate in proof-of-concept experiments that it is suitable for the clinical laboratory and can provide new insights into the host infection response.

Microscale versus macroscale protocols facilitate greater control over experimental conditions, ensure that all cells are uniformly exposed, are automatable, and can process small samples. Our cassette achieves complete erythrocyte lysis within 10-s exposure of whole blood to deionized water, exposes all cells to identical conditions via microridge-induced mixing, and limits stress-induced leukocyte activation, via their immediate return to isotonic conditions following lysis. Furthermore, the samples and reagents are automatically and precisely metered; all leukocyte subpopulations are efficiently recovered due to constant flow that prevents sedimentation. Furthermore, this system achieves ~25% increased total recovery versus a widely used macroscale method and can process samples from 10 μ L to several milliliters.

A leukocyte isolation method should efficiently yield all leukocyte subpopulations, with these cells accurately reflecting the activation state of the cells prior to processing. To this end, microfluidics-isolated cells are far more representative of the leukocytes in starting blood samples as opposed to macroscale isolated cells. Indeed, the microfluidics leukocytes show greatly increased intersample consistency both for naïve blood and for blood stimulated ex vivo with *Staphylococcal* enterotoxin B, which mimics the cellular effects of infection. Significantly, phenotypic analysis demonstrates these two populations are far more different from each other than seen between the macroscale populations. To this end, our microfluidics system facilitates the collection of previously unattainable data.

To assess phenotype, the samples were fixed on chip immediately after lysis, and leukocyte subpopulations were analyzed for high expression of cell surface activation markers, such as integrins. For granulocytes, at most 3% of the naïve cells score activated. Furthermore, these cells are highly responsive to SEB, with up to 80% scoring activated following 2-h SEB exposure. While granulocyte response is thought to be stimulated via cytokines from activated lymphocytes,²⁵ the rapid response seen here suggests SEB might directly stimulate these cells. In contrast, up to 25% of the naïve macroscale granulocytes score activated, and these cells are largely refractile to ex vivo SEB stimulation.

As the microfluidics cassette has been developed to evaluate transcriptome profiles in healthy versus trauma patients in different clinical centers, it is essential leukocyte isolation not introduce artifactual changes that mask genomic response to injury. The principal component plot in Figure 5A shows that

cassette lysis yields high signal-to-noise data. Supervised hierarchical clustering of differentially expressed genes reveals dramatic differences in leukocyte gene expression minus and plus SEB, with 1565 probe sets showing changes. These results demonstrate ex vivo SEB reprograms leukocyte gene expression, with significant upregulation of interleukins, chemokines, and cell surface receptors and downregulation of cell maintenance activities. Interestingly, the majority of the highly downregulated genes encode unknown functions. The appreciable absence of erythrocyte- and platelet-specific mRNAs indicates their highly efficient exclusion by microfluidics lysis. The genomic response to SEB challenge can provide insights into deleterious host activities accompanying infection. Accurate dissection of this response requires isolation of leukocytes that reflect their initial state in the blood.

In conclusion, the microfluidics cassette and water lysis protocol achieve erythrocyte-free, nonactivated leukocytes from whole blood for phenotype and global gene expression studies. This system facilitates the collection of reliable and highly robust data. Clinical centers have begun to implement this system to isolate leukocytes from burn and trauma patients, to produce global gene expression data that provide insights into trauma pathophysiology and new assessment and treatment protocols.

ACKNOWLEDGMENT

These studies were supported by the National Institute of Health, Inflammation and the Host Response to Injury Large Scale Collaborative Project, U54 GM-062119, and the National Institute of Health BioMEMS Resource Center P41 grant, P41 EB-002503. P.A.E. was supported by a T32 training grant, T32 GM-008721, for burn and trauma research. We thank Dr. Scott E. Stachel (BioDiversity LLC, Jackson, WY) for comments and editing, and Sandra MacMillan for outstanding technical assistance. Additional participating investigators in the Large Scale Collaborative Research Program entitled, "Inflammation and the Host Response to Injury" are as follows: Henry V. Baker, Paul E. Bankey, Timothy R. Billiar, Bernard H. Brownstein, Steve E. Calvano, David G. Camp II, Celeste Campbell-Finnerty, George Casella, Irshad H. Chaudry, Mashkoor Choudhry, J. Perren Cobb, Ronald W. Davis, Asit De, Constance Elson, Bradley Freeman, Richard L. Gamelli, Nicole S. Gibran, Douglas L. Hayden, Brian G. Harbrecht, David N. Herndon, Jureta W. Horton, William Hubbard, Jeffrey Johnson, Matthew B. Klein, James A. Lederer, Tanya Logvinenko, Stephen F. Lowry, Ronald V. Maier, John A. Mannick, Philip H. Mason, Grace P. McDonald-Smith, Bruce A. McKinley, Carol Miller-Graziano, Joseph P. Minei, Ernest E. Moore, Frederick A. Moore, Avery B. Nathens, Grant E. O'Keefe, Laurence G. Rahme, Daniel G. Remick, David A. Schoenfeld, Michael B. Shapiro, Martin Schwacha, Geoffrey M. Silver, Richard D. Smith, John Storey, H. Shaw Warren, Michael A. West, and Wenzhong Xiao.

Received for review January 18, 2006. Accepted April 28, 2006/

AC060140C

(25) Moulding, D. A.; et al. *Infect. Immun.* **1999**, *67*, 2312–2318.